Journal of Alloys and Compounds 507 (2010) 551–556

Contents lists available at ScienceDirect

Journal of Alloys and Compounds

journal homepage: www.elsevier.com/locate/jallcom

Memory switching of $ZnGa_2Se_4$ thin films as a new material for phase change memories (PCMs)

I.S. Yahia*, M. Fadel, G.B. Sakr, S.S. Shenouda

Physics Department, Faculty of Education, Ain Shams University, Roxy, Cairo, Egypt

ARTICLE INFO

Article history:
Received 10 May 2010
Received in revised form 4 August 2010
Accepted 5 August 2010
Available online 13 August 2010

Keywords:
Defect chalcopyrite semiconductor
$ZnGa_2Se_4$
Thin films
Dc electrical conductivity
Memory switching
Current–voltage characteristics
Electrothermal model

ABSTRACT

$ZnGa_2Se_4$ thin films were prepared by using thermal evaporation technique. X-ray diffraction patterns revealed the amorphous nature of the as- deposited films. The dc conductivity was studied as a function of temperature and thickness. The obtained results of dc electrical conductivity showed its semiconductor behavior and can be explained according to Mott and Davis model. The conduction activation energy ΔE_σ has one value for each thickness indicating the presence of one conduction mechanism through the studied range of temperature. Both dynamic and static *I–V* characteristic curves of amorphous $ZnGa_2Se_4$ thin films for switching and memory behavior have been studied as a function of thickness in the range (136–260 nm) and temperature in the range (305–373 K). *I–V* characteristic curves showed a memory switching at the threshold point [turnover point (TOP)] from the high resistance state (OFF state) to the low resistance state (ON state). The mean value of threshold voltage $\bar{V}_{th}$ increases linearly with increasing the film thickness while decreases exponentially with the increase of temperature. The mean value of the threshold electrical field $\bar{E}_{th}$ decreases exponentially with increasing temperature. The values of threshold activation energy ε and threshold resistance activation energy ΔE_R were calculated. The rapid transitions between the high resistive and conductive states were attributed to an electrothermal model initiated from Joule heating of current channel.

1. Introduction

The switching phenomenon is one of the numerous interesting effects arising in strong electric field [1]. The phenomenon has been observed in a great number of crystalline, amorphous and liquid semiconductors [2–4]. There are two types of electrical switching observed in amorphous semiconductors, namely threshold and memory-type. The threshold switching is considered as an electronic process and occurs when the charged defect states present in the glass are filled by field injected charge carriers. Memory switching, on the other hand, is believed to be a thermal process, which involves phase transformation of the material in the conducting channel, from amorphous to crystalline state [5]. In the threshold-type, the ON state persists only while a current flows down to a certain holding voltage, whereas in the memory-type, the ON state is permanent until a suitable reset current pulse is applied across the sample. Different mechanisms have been proposed to explain the phenomenon of electrical switching in amorphous semiconductors [6]. They include pure electronic [7], electrothermal [8] and thermal [9,10] mechanisms. It is more or less accepted that threshold switching is generally electronic in origin, whereas the memory switching is thermal in origin [11]. The formation of highly conducting crystalline channels or filaments is considered as a possible cause of memory switching in the amorphous semiconductors [12–13]. Dc electrical conductivity measurements provide information on the conduction process for studied device. Determination of the conduction mechanisms and the other electrical parameters is believed to be useful for improving the stability characteristics of the devices based on $ZnGa_2Se_4$ films.

Phase change random access memory (PCRAM) is one of the most promising candidates for the next-generation non-volatile solid-state memory due to its excellent features, such as low latency, high endurance, long retention and high scalability. PCRAM has many advantages, for example, non-volatility, high scalability, high speed, low power consumption, low cost and compatibility with complementary metal–oxide semiconductor (CMOS) technology. The memory-switching effect in phase change materials is achieved by pulsed electric fields to induce Joule heating, which leads to two distinct electronic states corresponding to amorphous and crystalline phases [14–16].

In the recent years, a great deal of interest has been focused on the defect chalcopyrite tetragonal $II–III_2–VI_4$ compounds. This interest has been driven by their possibility in semiconductor device applications. $ZnGa_2Se_4$ is among the poorly studied defect

* Corresponding author. Tel.: +20 182848753; fax: +20 222581243.
E-mail addresses: dr_isyahia@yahoo.com, isyahia@gmail.com (I.S. Yahia).

0925-8388/$ – see front matter © 2010 Elsevier B.V. All rights reserved.
doi:10.1016/j.jallcom.2010.08.021

chalcopyrite compounds in thin film form. The defect in this compound arises from some percentage vacancies of Zn sites which are expected to influence the physical properties of $ZnGa_2Se_4$ films. These semiconductors have considerable potential for device applications owing to their high photosensitivity and bright photoluminescence [17,18], combined with the long-term stability of many parameters and wide band gap semiconductor [19].

The aim of the present work is to study the dc conductivity and switching phenomena of $ZnGa_2Se_4$ thin films as a defect chalcopyrite compound for phase change optical memories. Also, the parameters affecting the switching voltage and the switching mechanism were extracted.

2. Experimental details

Bulk $ZnGa_2Se_4$ was prepared by the melt and slowly cooled technique using different heat treatments. The constituent elements of the investigated compound Zn, Ga and Se of high purity (5N), were weighed according to their stoichiometric ratio and sealed into an evacuated silica tube (10^{-5} Torr) and then heated in an especially designed oscillatory furnace. The temperature of the furnace was raised in steps up to 303 K (the melting point (m.p.) of Ga) at rate 100 °C/h and was kept at this value for 2 h. Then, it was raised at the same rate to 490 K (the m.p. of Se) followed by an increase up to 693 K (the m.p. of Zn). Finally, the furnace temperature was gradually raised by the same rate to 1423 K and kept at this temperature for 2 h. Then, the sample was gradually cooled down step by step until it reached the following temperatures 873, 773 and 643 K and kept for 1 h at each temperature [20]. Then, the sample was finally slowly cooled by the same rate of rising to the room temperature. The long duration of synthesis and the continuous mechanically shaking of the melt in the oscillatory furnace ensuring the high homogeneity of the investigated compound. Previous experience indicates that, this procedure usually gives the bulk samples showing a good polycrystalline structure [21].

Thin film samples of $ZnGa_2Se_4$ with different thicknesses were prepared by thermal evaporation technique, using a high vacuum plant (Edward's E 306A) onto a highly polished pyrographite and glass substrates held at room temperature. The synthesized ingot of the prepared system was crushed into small pieces. These pieces were put into a cleaned dry quartz boat placed inside a helical tungsten wire as an evaporation source. The distance between the source of material and the substrate holder was about 20 cm. The vacuum chamber was pumped down to 2×10^{-5} Torr. The temperature of the composition grains was then raised until the whole material evaporated with a deposition rate of about 10 nm/s. Samples of different thicknesses were prepared under the same evaporation conditions. The film thickness was controlled by using the thickness monitor (Edward FTM5), and then detected accurately by employing Tolansky's method of multiple-beam Fizeau fringes [22].

The film amorphicity was checked using X-ray diffraction pattern. Philips X-ray diffractometer (model X'-Pert) was used for the measurement by utilizing monochromatic CuKα radiation operated at 40 kV and 25 mA. The diffraction patterns were recorded automatically with a scanning speed of 2°/min.

For dc electrical conductivity, the as-deposited films were sandwiched between two Al electrodes and measured through a special designed holder. The electrical resistance of the investigated films was measured as a function of temperature using the high impedance digital electrometer (Keithly E 616A). Measurements of the current–voltage (*I–V*) characteristics were carried out in a special designed cell fitted with two electrodes, the lower one was a circular brass disk in contact with the pyrographite substrate and the upper electrode was a movable platinum wire with a thin circular end of diameter ≈200 micron to provide a gentle and good contact with the upper surface of the film by a weak spring. The pressure provided by the upper electrode as well as a point of contact was kept constant throughout the measurements [23]. The current–voltage *I–V* characteristics at different elevated temperatures were measured using a high impedance digital electrometer (Keithly E 616A) for the potential drop measurements and a microdigital multimeter (HC-5010-EC) for the current measurements passing through the sample. Heating system for the studied samples was controlled by a calibrated Chromel–Alumel thermocouple connected to a temperature controller in a close proximity to the sample.

3. Results and discussion

3.1. X-ray diffraction characterization

Fig. 1 shows the XRD spectra for the as-deposited $ZnGa_2Se_4$ films of different thicknesses. This figure revealed that there is no evidence of sharp lines corresponding to the crystallization, ensuring the amorphous nature of the prepared films.

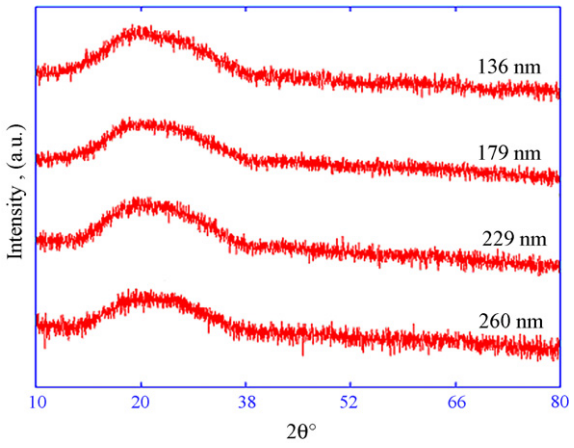

Fig. 1. X-ray diffraction pattern of $ZnGa_2Se_4$ thin films of different thicknesses.

3.2. Temperature dependence of the dc electrical conductivity for $ZnGa_2Se_4$ thin films

The experimental dc conductivity was studied for $ZnGa_2Se_4$ thin films in the temperature range (303–423 K) and in the thickness range (136–260 nm). Electrical resistance was measured as a function of temperature and thickness. The dc conductivity was calculated according to the following equation:

$$\sigma_{dc} = \frac{d}{RA}, \tag{1}$$

where R is the resistance of the sample, d is the sample thickness and A is the cross-section area of the parallel surface of the sample. Values of the conduction activation energy ΔE_σ and the pre-exponential factor σ_o of the as-deposited thin films were calculated according to the well-known Arrhenius's equation:

$$\sigma_{dc} = \sigma_o \exp\left(\frac{-\Delta E_\sigma}{k_B T}\right), \tag{2}$$

where k_B is the Boltzman's constant. Fig. 2 shows the relation between $\ln \sigma_{dc}$ and $1000/T$. The relation yields straight lines. The values of ΔE_σ, σ_o and σ_{RT} for each thickness were deduced and given in Table 1.

From Table 1, it is clear that the conduction activation energy ΔE_σ is independent of film thickness and its value equals ≈0.72 eV indicating the presence of one conduction mechanism through the

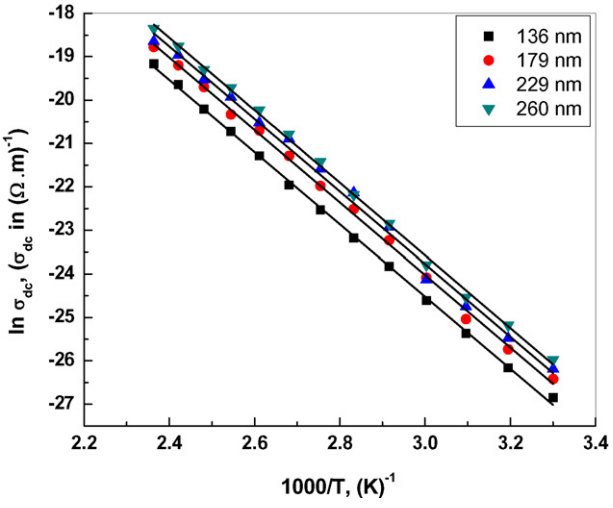

Fig. 2. Temperature dependence of dc electrical conductivity of $ZnGa_2Se_4$ thin films.

Table 1
Values of ΔE_σ, σ_o and σ_{RT} for each thickness.

d (nm)	ΔE_σ (eV)	σ_o $(\Omega\,m)^{-1}$	σ_{RT} $(\Omega\,m)^{-1}$
136	0.717	1.50	2.19×10^{-12}
179	0.719	2.75	3.36×10^{-12}
229	0.720	3.63	4.24×10^{-12}
260	0.721	4.49	5.25×10^{-12}

studied temperature range. It is found that σ_o and σ_{RT} increase with increasing the film thickness. This is because the density of lattice defects as vacancies, interstitials and dislocations, developed during the deposition of thin film are lowered with the increase of film thickness. Thus, film resistance is decreased and the conductivity is increased with the film thickness [24]. According to Mott and Davis [25], the activation energy alone does not provide any indication to whether the conduction takes place in the extended states near the mobility edge or by hopping in the localized states. This is because of the fact that both these conduction mechanisms can occur simultaneously with the conduction via local states dominating at lower temperature. The activation energy at the former case represents the energy difference between the mobility edge and the Fermi level, $E_C - E_F$ or $E_F - E_V$, while in the later case; it represents the sum of the energy separation between the occupied localized states and the Fermi level, $E - E_F$, and the mobility activation energy for the hopping process between the localized states. In order to obtain a clear distinction between these two conduction mechanisms, Mott and Davis [26] have suggested that the value of the pre-exponential factor σ_o corresponding to hopping in the extended states is expected to be $10^4\,(\Omega\,m)^{-1}$, while hopping conduction in the localized states at the band edges is lower by a factor 10^2–10^4. Therefore, the obtained data of ΔE_σ and σ_o for the investigated compound may be interpreted due to electrons hopping in the localized states of the band tail [27–29].

3.3. Switching properties of $ZnGa_2Se_4$ thin films

3.3.1. Dynamic and static I–V characteristics

The dynamic *I–V* characteristic curve displayed on the screen of a Cathode Ray Oscilloscope (CRO) using an ac source electrical circuit for $ZnGa_2Se_4$ film of thickness 229 nm (as an illustrative example) is presented in Fig. 3(A). This is a typical characteristic of a memory-switching device.

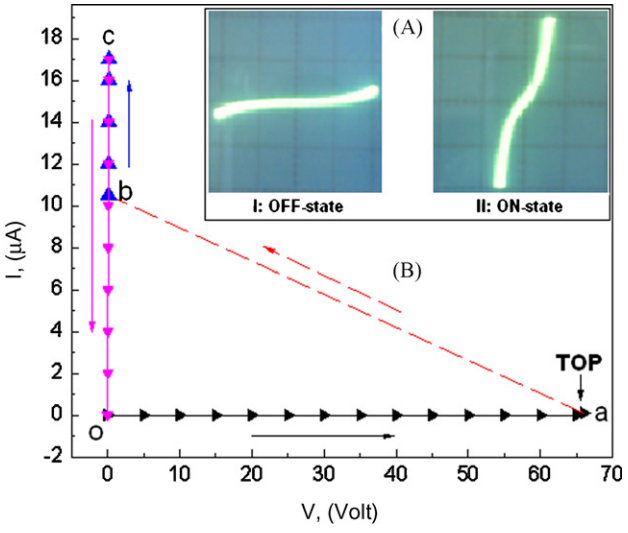

Fig. 3. Dynamic (A) and Static (B) *I–V* characteristics of $ZnGa_2Se_4$ thin film of thickness 229 nm (as a representative example).

Fig. 3(B) shows the static *I–V* curve using dc source for the same film thickness at room temperature. It is observed that the increase of the applied voltage to a critical or threshold voltage V_{th}, produced a very small current forming the first branch (part (oa): OFF state with a high resistance) of the switch. At point (a), the sudden increase in current and drop in voltage to the point (b) in a very short time of the order 10^{-9} s took place. Therefore, no data points are taken in this range (ab). A further increase in the applied voltage increases the current without any significant increase in the potential drop (part (bc): the ON state or the holding branch, with low resistance). On decreasing the applied voltage in this state, the current decreases until finally both become zero (part co). The obtained curve is a typical *I–V* characteristic for a memory switch. This behavior was observed in the investigated ranges of temperature and thickness as shown in Fig. 4. It is observed that there is a weaker appearance of the negative differential resistance (NDR) region of the *I–V* characteristics at higher temperatures.

3.3.2. Thickness and temperature dependencies of the threshold voltage $\bar{V}_{th}$

Fig. 5 illustrates the dependence of the mean value of the threshold voltage $\bar{V}_{th}$ on the film thickness. It is observed that $\bar{V}_{th}$ increases linearly with the film thickness. The observed relation between the thickness and $\bar{V}_{th}$ agrees well with the previous observations for different amorphous semiconductor materials [30,31]. Fig. 6 depicts the dependence of the threshold voltage on the temperature in the investigated thickness range. It was found that $\bar{V}_{th}$ decreases exponentially with the increase of temperature. This behavior is similar to those reported in literature [10,30,32]. If the ambient temperature increases, the thermal energy required for the transformation of the channel material (filament) from the amorphous to crystalline state will be lower. Therefore, the magnitude of the threshold voltage $\bar{V}_{th}$ decreases with increasing the ambient temperature [6]. Plots of ln $\bar{V}_{th}$ versus $1000/T$ for the studied $ZnGa_2Se_4$ samples are presented in the inset of Fig. 6. The straight lines obtained by least square fitting satisfy the following Arrhenius formula [11]:

$$V_{th}(T) = V_0 \exp\left(\frac{\varepsilon}{k_B T}\right), \tag{3}$$

where V_0 is a constant and ε is the threshold activation energy which can be deduced by least square fitting and given in Table 2.

The temperature dependence of the threshold voltage can be explained in terms of an electrothermal model [10,33]. Since, the temperature of the semiconductor is raised due to Joule heating and the conduction process in an amorphous material is an activated type [34]. So, the conductivity of the sample will increase due to the effect of heating. This will allow more current to flow through the heated region and allow more Joule heating, resulting in a further increase in the current density. Ultimately, the temperature rise will become adequate to initiate the thermal breakdown owing to the strong temperature dependence of the conductivity. A stationary state is reached when the heat lost by conduction from the current filament becomes equal to the Joule heat generated in that region. Finally, it is suggested that the memory-switching phenomenon is caused by a phase transition of the material from glassy to crystalline state due to Joule heating, and can be understood in terms of the electrothermal process [35].

The threshold field $\bar{E}_{th}(T) = \bar{V}_{th}/d$ (d is the film thickness) has been deduced at the TOP. The dependence of the $\bar{E}_{th}$ on temperature of the active region is plotted in Fig. 7. It is clear that $\bar{E}_{th}$ decreases with increasing temperature and increases with increasing the film thickness.

The calculated values of R_{th} at different temperatures are obtained from the values of $\bar{V}_{th}$ and $\bar{I}_{th}$. Plots of ln R_{th} versus $1000/T$ are presented in Fig. 8. The straight lines obtained by least square

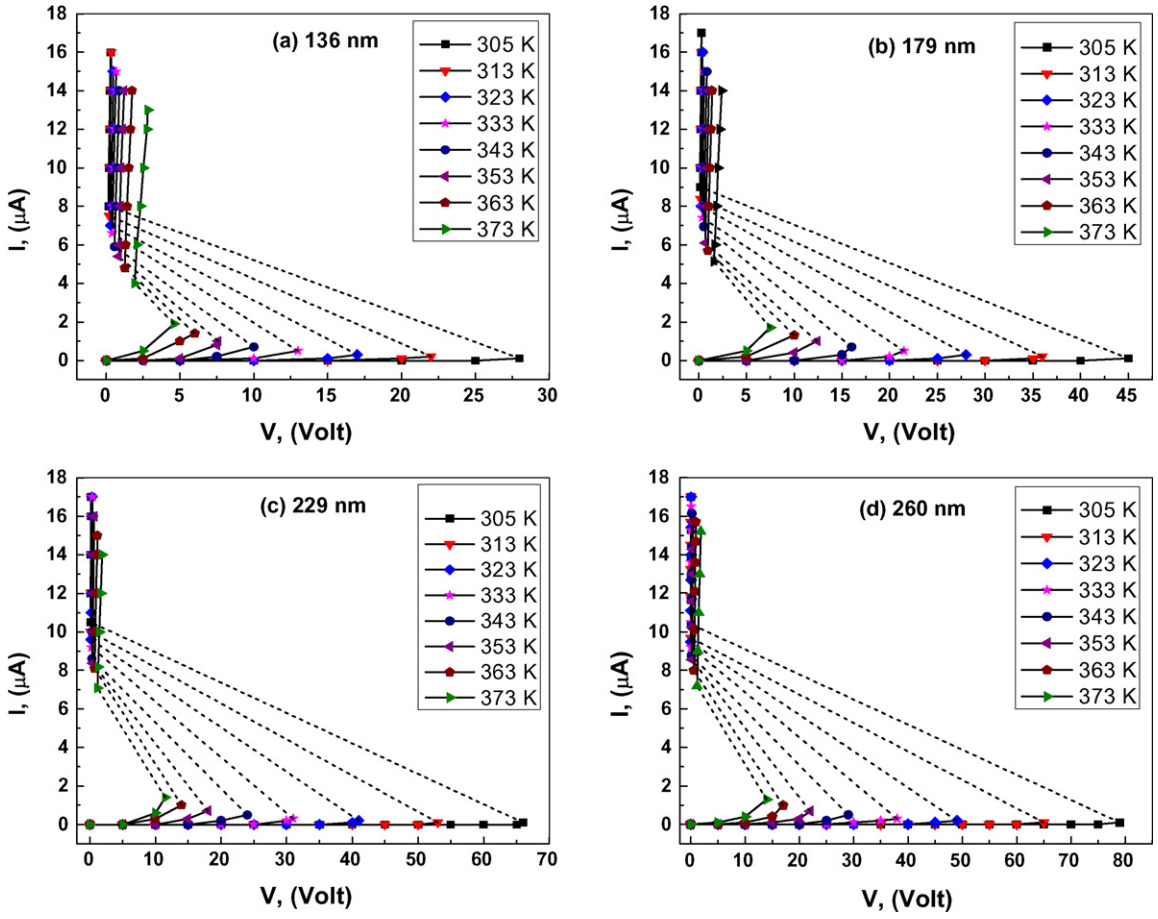

Fig. 4. *I–V* characteristic curves of $ZnGa_2Se_4$ thin films of different thicknesses.

fitting satisfy the following equation [36]:

$$R_{th}(T) = R_0 \exp\left(\frac{\Delta E_R}{k_B T}\right), \quad (4)$$

where ΔE_R is the threshold resistance activation energy which can be deduced by least square fitting and given in Table 2. It is observed that the values of ΔE_σ and ΔE_R are approximately in the same order.

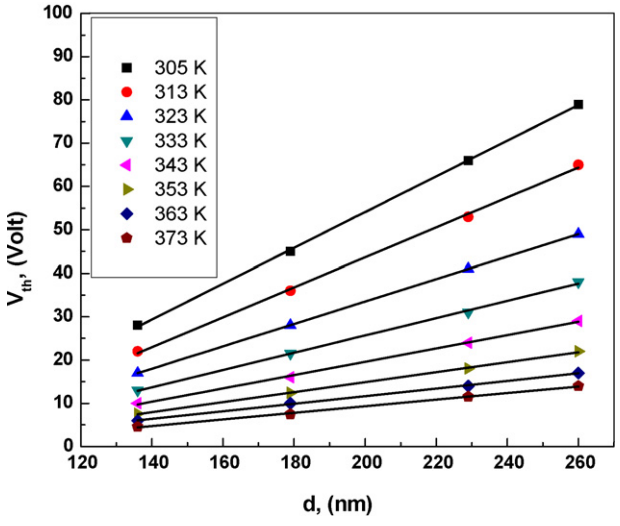

Fig. 5. Thickness dependence of threshold voltage $\bar{V}_{th}$ of $ZnGa_2Se_4$ thin films.

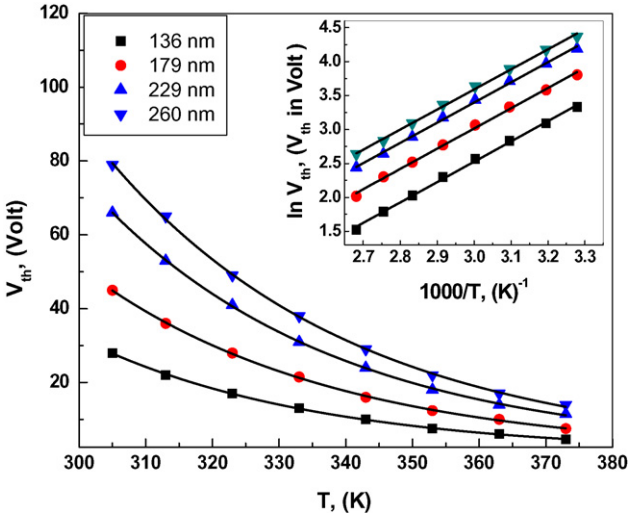

Fig. 6. Temperature dependence of threshold voltage $\bar{V}_{th}$ of $ZnGa_2Se_4$ thin films. Inset: Plot of ln $\bar{V}_{th}$ versus 1000/*T*.

Table 2
Values of ε, ΔE_R and $\varepsilon/\Delta E_\sigma$ for $ZnGa_2Se_4$ thin films.

Thickness	ε (eV)	ΔE_R (eV)	$\frac{\varepsilon}{\Delta E_\sigma}$
136	0.259	0.667	0.361
179	0.257	0.652	0.357
229	0.256	0.664	0.355
260	0.255	0.656	0.354

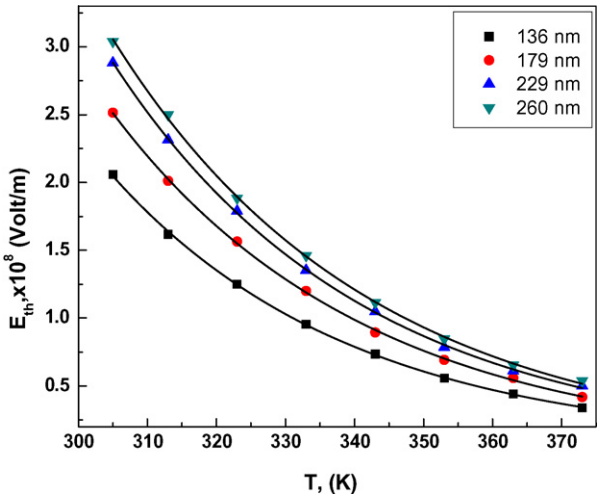

Fig. 7. Temperature dependence of threshold field $\bar{E}_{th}$ of $ZnGa_2Se_4$ thin films.

The electrothermal model can be solved to a certain extent by finding a stationary state solution for the heat transport equation [37]:

$$C\left(\frac{dT}{dt}\right) = \nabla\cdot(\Psi\nabla T) + E_{th}^2\sigma_{dc}, \quad (5)$$

where C is the heat capacity, ψ is the thermal conductivity coefficient of the sample. The charge conservation equation is [38]:

$$\nabla E = \frac{-1}{\sigma_{dc}}\left(\frac{d\rho}{dt}\right), \quad (6)$$

where ρ is the charge density. Several simplifications are commonly introduced which explain the thermal breakdown. In the case of steady state breakdown, dT/dt can be neglected for the solution of Eq. (5), then the heat conduction equation for a small difference $\Delta T_{breakdown} = T_m - T_s$, between the temperature of the middle of the specimen T_m and on its surface T_s (the studied ambient temperature) becomes [10]:

$$8\psi\left(\frac{\Delta T}{d^2}\right) + E_{th}^2\sigma_{dc} = 0, \quad (7)$$

This means that heat conduction is balanced by Joule heating. Breakdown occurs when the amount of heat generated by Joule heating in the specimen cannot be removed by thermal conduction. The temperature difference of the breakdown $\Delta T_{breakdown}$ obtained with the help of Eqs. (2) and (7) is given by [10]:

$$\Delta T_{breakdown} = \frac{T_s^2 k_B}{\Delta E_\sigma}, \quad (8)$$

For the switching process, the temperature inside the active region of the specimen as a function of the generated power p_{th} is given by the relation [39]:

$$T_m = T_s + \frac{p_{th}}{2\pi d\psi}, \quad (9)$$

and so,

$$\Delta T_{breakdown} = \frac{p_{th}}{2\pi d\psi}, \quad (10)$$

According to Eq. (8), the values of $\Delta T_{breakdown}$ were calculated at different temperatures and given in Table 3.

It can be noticed that $\Delta T_{breakdown}$ increases simultaneously with the ambient temperature, and this agrees with different amorphous semiconductor materials [32,38,40]. Also, the thickness dependence of the $\Delta T_{breakdown}$ is weak because the values of the electrical activation energy are approximately constant with the film thickness. According to Eq. (10), the thermal conductivity for each thickness can be calculated and the mean value at the room temperature is found to be 0.375 W/(m K).

The values of the temperature at the middle of the specimen can be calculated according to $T_m = T_s + \Delta T_{breakdown}$. It was observed that T_m increases linearly with T_s as shown in Fig. 9, which may be attributed to the increase of the vibrational amplitude of the network atoms. Consequently, the number of collisions between the

Table 3
Values of $\Delta T_{breakdown}$ for $ZnGa_2Se_4$ thin films.

T_s (K)	$\Delta T_{breakdownnm}$ (K)			
	136 nm	179 nm	229 nm	260 nm
305	11.190	11.159	11.144	11.128
313	11.785	11.752	11.736	11.720
323	12.550	12.515	12.498	12.480
333	13.339	13.302	13.283	13.265
343	14.152	14.113	14.093	14.074
353	14.990	14.948	14.927	14.906
363	15.851	15.807	15.785	15.763
373	16.736	16.690	16.666	16.643

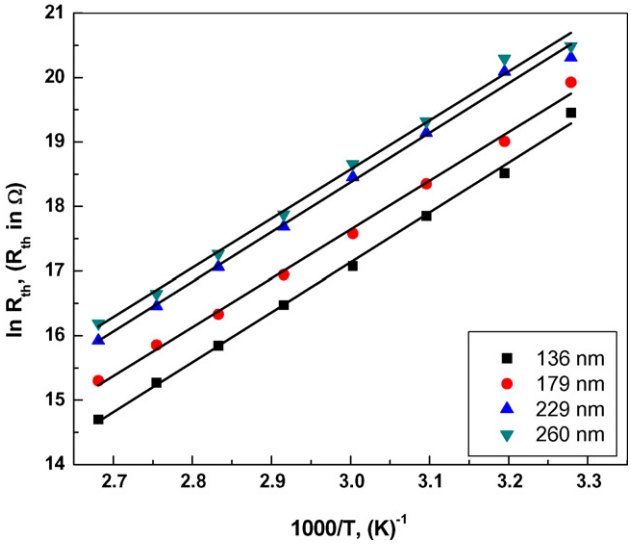

Fig. 8. Plot of $\ln R_{th}$ versus $1000/T$ of $ZnGa_2Se_4$ thin films.

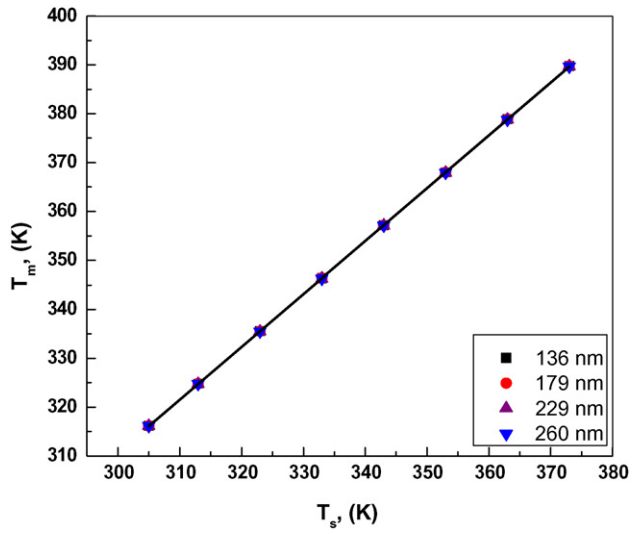

Fig. 9. Plot of T_m versus T_s of $ZnGa_2Se_4$ thin films.

charge carriers and the network atoms increases, which may interpreted by increasing $\Delta T_{breakdown}$ with the ambient temperature as given in Table 3.

The higher values $\Delta T_{breakdown}$ reported by Armitage et al. [41], Shimakawa et al. [38] and Böer and Ovshinsky [42] supported the thermal model. While, in this work, the values of $\Delta T_{breakdown}$ are very small. Therefore, the calculated values of $\Delta T_{breakdown}$ and $\varepsilon/\Delta E_{th} < 0.5$ support the electrothermal model to interpret the switching conduction mechanism for $ZnGa_2Se_4$ thin films.

4. Conclusions

$ZnGa_2Se_4$ as defect chalcopyrite was successfully grown by thermal evaporation technique. The X-ray diffraction patterns showed that the as-deposited films posses the amorphous nature. The conduction activation energy ΔE_σ has a single value for each thickness indicating the presence of one conduction mechanism through the studied range of temperature. The obtained results of dc conductivity were interpreted by Mott and Davis model due to electrons hopping in the localized states of the band tail. Dynamic and static *I–V* characteristic curves for the studied films are typical for a memory-switching device. The mean value of the threshold voltage $\bar{V}_{th}$ increases linearly with increasing the film thickness and decreases exponentially with the increase of the temperature. Also, the threshold field $\bar{E}_{th}$ decreases exponentially with increasing temperature. The values of threshold activation energy ε and the threshold resistance activation energy ΔE_R were calculated. Values of the temperature difference inside and on the surface of the film were increased simultaneously with the ambient temperature. The data obtained for the switching characteristics were interpreted by the electrothermal model based on the low values of $\Delta T_{breakdown}$ and the ratio $\varepsilon/\Delta E_\sigma$ which is found to be less than 0.5.

References

[1] R. Lokesh, N.K. Udayashankar, S. Asokan, J. Non-Cryst. Solids 356 (2010) 321–325.
[2] M.M. Nassary, S.A. Hussein, A.T. Nagat, Cryst. Res. Technol. 29 (1994) 869.
[3] M.A. Afifi, N.A. Hegab, A.E. Bekheet, E.R. Sharaf, Physica B 404 (2009) 2172–2177.
[4] A.A. Al-Ghamdi, A.T. Nagat, F.S. Bahabri, R.H. Al-orainy, S.R. Al-harbi, F.S. Al-Hazmi, J. Alloys Compd. 484 (2009) 561–566.
[5] B.J. Madhu a, H.S. Jayanna a, S. Asokan, J. Non-Cryst. Solids 355 (2009) 2630–2633.
[6] M.P. Slankamenac, S.R. Lukić, M.B. Živanov, Semicond. Sci. Technol. 24 (2009) 085021.
[7] D. Adler, M.S. Shur, M. Silver, S.R. Ovshinsky, J. Appl. Phys. 51 (1980) 3289.
[8] D. Adler, Sci. Am. 36 (1977) 236.
[9] H. Fritzsche, S.R. Ovshinsky, J. Non-Cryst. Solids 4 (1970) 464.
[10] R. Mehra, R. Shyam, P.C. Mathur, J. Non-Cryst. Solids 31 (1979) 435.
[11] R. Rajesh, J. Philip, Semicond. Sci. Technol. 18 (2003) 133.
[12] H. Fritzsche, IBM J. Res. Dev. 13 (1969) 515.
[13] M. Dominguez, E. Marquez, P. Villares, R. Jimenez-Garay, Semicond. Sci. Technol. 3 (1988) 1106.
[14] N. Papandreou, A. Pantazi, A. Sebastian, E. Eleftheriou, M. Breitwisch, C. Lam, H. Pozidis, Solid-State Electron. 54 (2010) 991–996.
[15] S.A. Kozyukhin, A.I. Popov, E.N. Voronkov, Thin Solid Films 518 (2010) 5656–5658.
[16] Yifeng Gu, Zhitang Song, Ting Zhang, Bo Liu, Songlin Feng, Solid-State Electron. 54 (2010) 443–446.
[17] Whe-Tek Kim, Chang-Sub Chung, Jong-Geum Kim, et al., Phys. Rev. B: Condens. Matter 38 (1988) 2166.
[18] M. Turowski, A. Kisiel, Solid State Phys. 17 (1984) 661.
[19] T.G. Kerimova, A.G. Sultanova, Inorganic Materials 38 (2002) 992, Translated from Neorganicheskie Materialy, 38 (2002) 1181, Original Russian Text Copyright © 2002 by Kerimova, Sultanova.
[20] M. Morocoima, M. Quintero, E. Guerrero, R. Tovar, P. Conflant, J. Phys. Chem. Solids 58 (1997) 503.
[21] E.A. El-Sayad, G.B. Sakr, Phys. Status Solidi (a) 201 (2004) 3061.
[22] S. Tolansky, Introduction to Interferometry, Longman, London, 1955.
[23] M.A. Afifi, H.H. Labib, N.A. Hegab, M. Fadel, A.E. Bekheet, Indian J. Pure Appl. Phys. 33 (1995) 129.
[24] M.A. Afifi, N.A. Hegab, H.E. Atyia, A.S. Farid, J. Alloys Compd. 463 (2008) 10.
[25] N.F. Mott, E.A. Davis, Electronic Process in Non-crystalline Materials, Clarendon Press, Oxford, 1971.
[26] E.A. Davis, N.F. Mott, Phil. Mag. 22 (1970) 903.
[27] J.B. Webb, D.E. Brodie, Can. J. Phys. 52 (1974) 2240.
[28] P.K. Lim, D.E. Brodie, Can. J. Phys. 55 (1977) 1512.
[29] P.K. Lim, D.E. Brodie, Can. J. Phys. 55 (1977) 1641.
[30] M.A. Afifi, N.A. Hegab, A.E. Bekheet, E.R. Sharaf, Physica B 404 (2009) 2172.
[31] M.A. Afifi, M.M. Abdel-Aziz, H.H. Labib, M. Fadel, E.G. El-Metwally, Vacuum 61 (2001) 45.
[32] M.M. Abdel-Aziz, Appl. Surf. Sci. 253 (2006) 2059.
[33] M. Anbarasu, S. Asokan, Appl. Phys. A 80 (2005) 249.
[34] H.J. De Wit, C. Crevecoeur, Solid State Electron. 15 (1972) 729.
[35] A.H. Abou El-Ela, N. Abdel Mohsen, H.H. Labib, Appl. Phys. A 26 (1981) 171.
[36] N.F. Mott, Phil. Mag. 22 (1970) 7.
[37] K. Shimakawa, Y. Inagali, T. Arizumi, Jpn. J. Appl. Phys. 12 (1973) 12.
[38] K. Shimakawa, Y. Inagaki, T. Arizum, Jpn. J. Appl. Phys. 11 (1972) 1319.
[39] T. Kaplan, D. Adler, J. Non-Cryst. Solids 8 (1972) 538.
[40] M.A. Afifi, N.A. Hegab, H.H. Labib, M. Fadel, Indian J. Pure Appl. Phys. 30 (1992) 211.
[41] D. Armitage, D.E. Brodie, P.C. Eastman, Can. J. Phys. 49 (1971) 1662.
[42] K.W. Böer, S.R. Ovshinsky, J. Appl. Phys. 41 (1970) 2675.